J. Mt. Sci. (2018) 15(3): 532-547
https://doi.org/10.1007/s11629-017-4692-5
e-mail: jms@imde.ac.cn
http://jms.imde.ac.cn

Detrital apatite fission track constraints on Cenozoic tectonic evolution of the northeastern Qinghai-Tibet Plateau, China: Evidence from Cenozoic strata in Lulehe section, Northern Qaidam Basin

DU Ding-ding[1,2] http://orcid.org/0000-0003-3553-3491; e-mail: dudd15@lzu.edu.cn

ZHANG Cheng-jun[1,2*] http://orcid.org/0000-0001-5030-7527; e-mail: cjzhang@lzu.edu.cn

MUGHAL Muhammad Saleem[1,2,3] http://orcid.org/0000-0002-7141-7300; e-mail: muhammadsaleem152@yahoo.com

WANG Xiao-yu[1,2] http://orcid.org/0000-0002-3425-4346; e-mail: wangxiaoyu@lzu.edu.cn

BLAISE Dembele [1,2] http://orcid.org/0000-0002-6836-2775; e-mail: blaise16@lzu.edu.cn

GAO Jun-ping[1,2] http://orcid.org/0000-0002-2623-2243; e-mail: 2975227654@qq.com

MA Yuan[1,2] http://orcid.org/0000-0002-6592-6782; e-mail: e-mail: 709333628@qq.com

LUO Xin-rong[1,2] http://orcid.org/0000-0002-1256-6832; e-mail: 286881284@qq.com

** Corresponding author*

1 School of Earth Sciences and Mineral Resources, Lanzhou University, Lanzhou 730000, China;

2 Key Laboratory of Western China's Mineral Resources of Gansu Province, Lanzhou 730000, China

3 Institute of Geology, University of Azad Jammu and Kashmir, Muzaffarabad 13100, Pakistan

Citation: Du DD, Zhang CJ, Mughal MS, et al. (2018) Detrital apatite fission track constraints on Cenozoic tectonic evolution of the northeastern Qinghai-Tibet Plateau, China: Evidence from Cenozoic strata in Lulehe section, Northern Qaidam Basin. Journal of Mountain Science 15(3). https://doi.org/10.1007/s11629-017-4692-5

Abstract: The Northern Qaidam Basin is located at the northeastern part of the Qinghai-Tibetan Plateau. It contains very thick Cenozoic terrestrial clastic sediments, which records the formation of the northern Qaidam Basin due to compressional deformation during the Indo-Asian collision. In this paper, we used detrital apatite fission-track thermochronology, including 4 sandstones and 2 conglomerates samples from the Lulehe section, to reveal the Cenozoic evolution of the northern Qaidam Basin. Fission-track dating indicated the source region of the Lulehe section has experienced important cooling and uplifting in the Late Cretaceous (at ~85.1 Ma and ~65 Ma) and the Eocene (~52 Ma), respectively. The AFT age distribution on the section suggested that the provenance of Lulehe section sediments were mainly derived from the south Qilian Shan (Qilian Mountains) and Altun Shan (Altun Mountains), and two significantly provenance changes may occur at 43.4-46.1 Ma and ~37.8 Ma, respectively. The results may have strong constrains on the Cenozoic deformation and tectonic evolution of the northern Qaidam Basin and Qinghai-Tibet Plateau.

Keywords: Northern Qaidam Basin; Apatite Fission-Track; Tectonic evolution; Provenance analysis

Received: 20 September 2017
Revised: 13 December 2017
Accepted: 01 February 2018

Introduction

Mostly rocks contain apatite as an accessory mineral. Fission tracks (FT) in apatite crystals form at known rates and can be used to calculate fission track ages (Naeser 1979; Zhang et al. 2009). Apatite fission track (AFT) lengths are related to thermal history of the rock and chemical composition of apatites (Crowley et al. 1991; Carlson et al. 1999). Therefore, the age and track length can record some information of tectonic-thermal evolution for the source rock (Gallagher et al. 1998; Wendt et al. 2002). Brandon et al. (1998) argued apatites are partially reset or unreset when the age is older than the depositional age. In addition, the youngest age group indicated that the source region have occurred a rapid cooling event or volcanic activity in the depositional profile. The lag time is a key factor to result in the difference between the youngest component and the depositional age (Garver et al. 1999; van der Beek et al. 2006; Rahl et al. 2007). In general, if the lag time is short, it reflects the source region have occurred tectonic activity and rapid erosion. Whereas if the lag time is long, it suggests that the source region underwent very slow exhumation when passing through the apatite partial annealing zone (APAZ: 60~110±10℃) (Garver et al. 1999).

The Northern Qaidam Basin (NQB) is located in the northeastern of the Tibetan Plateau (TP) (Roger et al. 2010), and the basin is an excellent approach to understand the uplifting mechanism of the TP due to continental collision between the Indian and Asian plates during Cenozoic (Liu et al. 2003). Most studies have concentrated on bedrock around the mountain (Jolivet et al. 2001; Sobel and Strecker 2003; Wang et al. 2004; Chen et al. 2006; Danišík et al. 2010; Anczkiewicz et al. 2013), while little thermochronologists who worked on sedimentary rocks in the basin (Emmel et al. 2006; Lin et al. 2016; Wang et al. 2016).

The thickness of Cenozoic detrital sediments in the NQB ranges from 4 to 5 km. These sediments can be used to identify the relationships between mountain uplifting, rock denudation and deposition processes (Wang 1997; Zhang et al. 2001; Yin et al. 2002; Ritts et al. 2004; Sun et al. 2005; Zheng et al. 2010; Zhuang et al. 2011b; Zhuang 2011; Lin et al. 2016; Wang et al. 2016). Plentiful studies have been carried out to understand tectonic activities and the provenance changes in the basins, among which the detrital AFT method is a powerful technique to find out provenance changes (Emmel et al. 2006; Green et al. 2006; Foster and Carter 2007; Olivetti et al. 2013; Yang et al. 2014; Zhang et al. 2015; Naylor et al. 2015; Lin et al. 2016; Oliveira et al. 2016; Wang et al. 2016). However, some research works were only limited to sedimentary facies and diagenetic process analysis (Sun et al. 2012; Chen et al. 2013; Sun et al. 2015; Chen et al. 2015), and others provenance analysis were confined to a few basic methods which are analysis of heavy minerals, paleocurrent and clastic particles grading in the NQB (Lin et al. 2014; Li et al. 2014; Li et al. 2015a; Li et al. 2015b; Liu et al. 2017). Moreover, most work on high accuracy provenance analysis was more concentrated in the western Qaidam basin (Zhou et al. 2012; Cheng et al. 2016). And thus the Lulehe section work seems to be more desperately needed.

The detrital AFT dating method has less been discovered similar study of the key Lulehe section in the NQB. This paper reported new ages integrated with previously published magnetostratigraphic ages (Zhang 2006) to find out the time of provenance change in the NQB, and thus to have a better understanding of the tectonic activity history of the NQB during the Cenozoic, by getting new evidences of formation and evolution of the Qinghai-TP. Meanwhile the present study also provides some rough information about the provenance direction in the Lulehe area.

1 Geological Setting and Stratigraphy

The study area is situated on the northeast of the Qaidam Basin, extending from NW to SE directions (Figure 1A). The area is bordered by Qilian Shan to the north, Qaidam Basin to the south and Kunlun Shan to the east. Altyn Tagh Fault (ATF), Northern Qaidam thrust fault belt (NQF) and Kunlun Fault (KLF) are forming borders of the Qaidam Basin (Wang et al. 2003; Wei et al. 2005; Yin et al. 2008a and b; Lu and Xiong 2009; Liu et al. 2012; Wang et al. 2017) (Figure 1B). NQB has some complex internal structures, including Lenghu fault system, Eboliang fault system, Jianshan fault system, Yahu

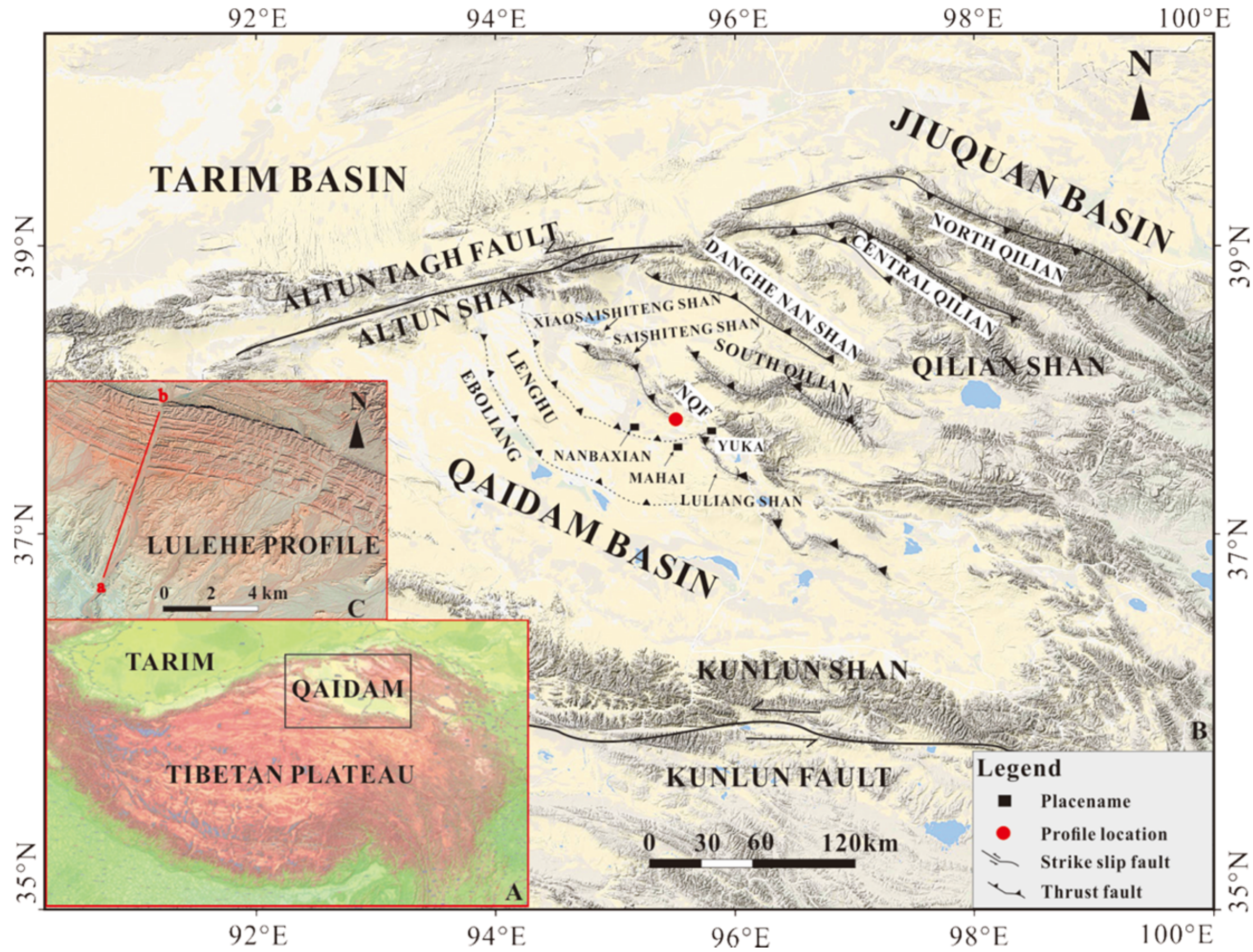

Figure 1 (A) Sketch map of the Tibet Plateau and adjacent region. (B) The major tectonic features around the northern Qaidam Basin. (C) Lulehe section map.

fault system and Nanbaxian fault system, and the fault systems can be further divided into several smaller fault (Yin et al. 2008a and b; Lu and Xiong 2009), (Figure 1B).

The area' s strata are complete, besides covering Mesozoic and Cenozoic strata inside the basin, the strata of the surrounding mountains area are well exposed from the Proterozoic to Quaternary. The bedrocks range from the Proterozoic to Paleozoic, whereas the Mesozoic rock is not developed (Figure 2). Cenozoic sedimentary is composed of lacustrine facies clastic rock and occasional thin layer algal limestone that is sandwiched between them (Chen and Bowler 1986), (Figure 2).

The NQB contains thick Cenozoic clastic sediments (thickness>4 km) that bear plentiful important information about the relationship between the basin and the surrounding mountains. The Cenozoic sediments at the western Qaidam Basin from bottom to top, can be subdivided into the Paleocene-early Eocene Lulehe Formation (53.47-42.8 Ma), the lower middle Eocene-late Eocene Xiaganchaigou Formation (42.8-31.5 Ma), and the upper early Oligocene Xiaganchaigou Formation (37.5-31.5 Ma) (Fang et al. 2007). Lithologic composition is given by pebbly sandstone, sandstone, argillaceous siltstone, silty mudstone and shale. Several unconformity layers suggested that there may be multiple tectonic activities occurred when the sediments deposited in the basin (Ren et al. 2004; Yin et al. 2008a and b; Li et al. 2012; Wang et al. 2017), (Figure 2). The Lenghu and Eboliang fault developed fan delta, alluvial fan and lake sedimentary system. Mahai-Nanbaxian area developed braided river delta, braided river, alluvial fan and lake depositional system (Yin et al. 2008a and b).

We studied the Lulehe section (Start: 38°08′05.26′′N, 94°41′18.25′′E; End: 38°06′23.99′′N,

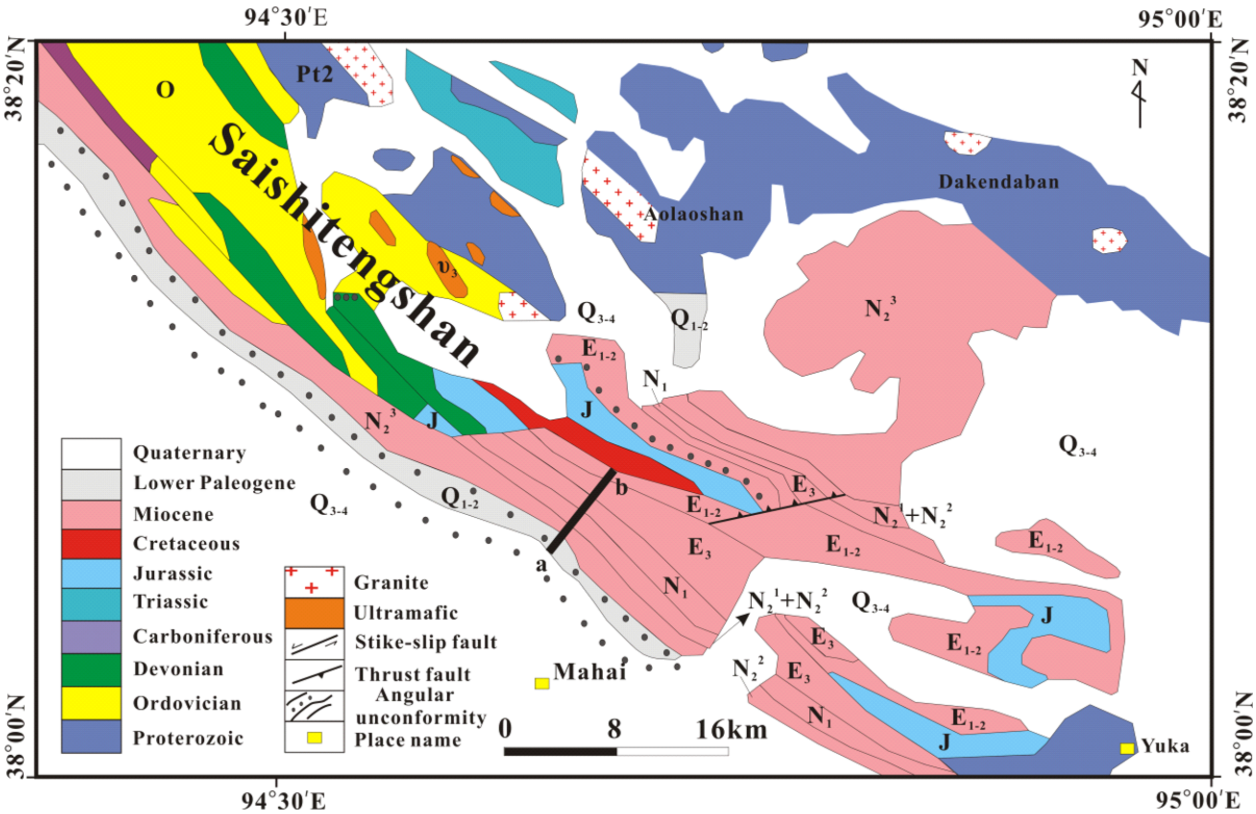

Figure 2 Geological sketch and the profile Lulehe district in the northern Qaidam Basin. a-b black line stands for Lulehe profile. N_1: Shangganchaigou Formation; N_2^1: Xiayoushashan Formation; N_2^2: Shangyoushashan Formation; N_2^3: Shizigou Formation; E_{1-2}: Lulehe Formation; E_3: Xiaganchaigou Formation; Q_{1-2}: Lower Pleistocene; Q_{3-4}: Middle Pleistocene-Holocene.

94°40′38.15′′E) in the south margin of the eastern Saishiteng Shan, which is located in the middle of the Qaidam Basin (Figures 1C and 2). The study area is about 30 km to the east of Yuka and about 18 km to the south of Mahai (Figure 2). Paleocurrent analysis showed that the Qilian and Altun systems were important sediment source area since the Cenozoic (Rieser et al. 2005; Yin et al. 2008a and b; Li et al. 2009; Lin et al. 2014) .

2 Materials and Methods

In the present study, 4 sandstones and 2 conglomerates samples, each one has a weight of about 2-3 kg, have been collected along Lulehe section from the Lulehe Formation to Xiaganchaigou Formation (Figure 3). Samples were crushed to obtain 0.25~0.05 mm debris, then processed by shaking standard magnetic heavy liquid separation techniques. More than 50 apatite grains were picked for each sample, and then these grains were mounted in using epoxy resin (Figure 4a). After polishing, the etching of grains was carried out by using 25% HNO_3 at 20 °C for 20 seconds (Figure 4b). The AFT dating was conducted at the Institute of High Energy Physics, Chinese Academy Of Sciences. All six samples were dated by the external detector method (Hurford 1983), using low-U mica external detectors which covered apatite grain mounts and glass dosimeters (CN5) during the irradiation. The age-calibration (ξ calibration) standard was used for apatite with personal zeta ξ=375±16 (Hurford and Green 1982; Yuan 2007). After doing irradiation, mica detectors were then etched in 45% HF (hydrofluoric acid) at 20 °C for 40 seconds to show the induced FTs. After this FT counting and track-length measurements were carried out with the help of Zeiss microscope using a magnification of 1000 with dry objectives for apatite. The data is listed in Table 1; ages of samples were taken with an error (±1σ). The annealing temperature of AFT is taken as ~110°C±10°C, and temperature of the APAZ is

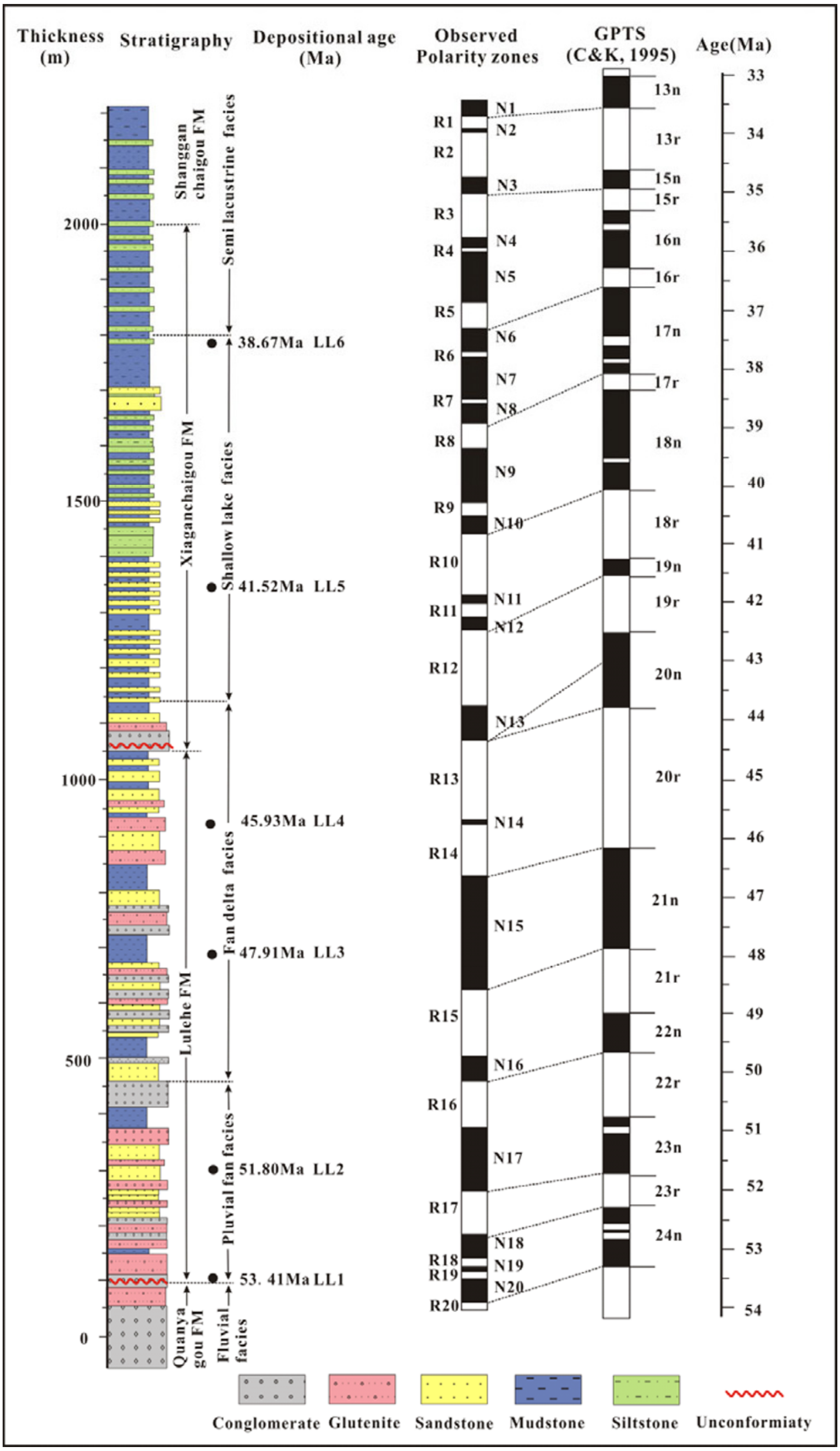

Figure 3 Comparison between magnetic polarity column in Lulehe profile and GPTS. The observed magnetic polarities are based on the results of Zhang (2006). GPTS (Cande and Kent 1995); Sampling site is the black spot.

Table 1 Result of AFT in Lulehe Profile in Northern Qaidam Basin

Sample number	Stratum	Mineral	n	Alt. (m)	$\rho_s(N_s)$ (10^5/cm)	$\rho_i(N_i)$ (10^5/cm)	$\rho_d(N_d)$ (10^5/cm)	U (ppm)	D_{par} (μm±1σ)	$P(x^2)$ (%)	Central age (Ma) (±1σ)
LL1	Lulehe Formation	Ap	46	096	1.676 (668)	12.699 (5062)	15.309 (16329)	14.3	1.81	97.4	38±2
LL2		Ap	37	306	3.385 (1609)	15.682 (7455)	15.499 (16329)	16.2	1.84	0	55±4
LL3		Ap	51	691	1.600 (879)	9.849 (5410)	15.688 (16329)	17.6	1.91	28.4	48±3
LL4		Ap	54	924	2.414 (1566)	15.347 (9957)	15.878 (16329)	18.3	1.82	30.4	46±3
LL5	Xiaganchaigou Formation	Ap	54	1334	3.480 (2041)	18.109 (10620)	16.067 (16329)	19.2	1.91	2.1	56±3
LL6		Ap	53	1782	4.111 (1644)	19.136 (7652)	16.256 (16329)	16.5	1.97	37.7	65±3

Sample number	Stratum	Mineral	n	Alt. (m)	Pooled age (Ma) (±1σ)	(N_l) Mean track length (μm)	Depositional Age (Ma)	Age range (Ma)	P1	P2	P3
LL1	Lulehe Formation	Ap	46	096	38±2	10.4±0.1 (104)	53.41	25.4-95.0	37.8 (46, W=100%)	xxx	xxx
LL2		Ap	37	306	62±3	10.7±2.1 (110)	51.80	23.4-94.6	25.1 (2.5, W=6.6%)	52 (28.3, W=76.6%)	85.1 (6.2, W=16.8%)
LL3		Ap	51	691	48±3	10.6±2.0 (111)	47.91	25.0-86.9	43.4 (41.3, W=81%)	65.3 (9.7, W=19%)	xxx
LL4		Ap	54	924	47±2	11.2±2.1 (114)	45.93	18.8-70.2	45.5 (N_f=50.6, W=93.8%)	64.6 (N_f=3.4, W=6.2%)	xxx
LL5	Xiaganchaigou Formation	Ap	54	1334	58±3	11.2±2.0 (109)	41.52	22.4-81.5	46.1 (N_f =25.4, W=47%)	63.5 (N_f =28.6, W=53%)	xxx
LL6		Ap	53	1782	65±3	11.6±2.1 (110)	38.67	36.5-100.8	56.9 (N_f =10.9, W=20.5%)	67 (N_f =42.1, W=79.5%)	xxx

Notes: n, number of apatite crystals analyzed per sample; Alt., Altitude; ρ_s, spontaneous track density in analyzed apatite crystals; ρ_i, induced track density in external detector for analyzed crystals; ρ_d, induced track density in external detector adjacent to dosimetry glass; N_s, number of spontaneous tracks counted; N_i, number of induced tracks counted; N_d, number of tracks counted in determining ρ_d; U, concentration (ppm); D_{par}, the fission-track etch pit measurements related to track length; $P(x^2)$, chi-square probability; N_l, number of measured confined track lengths. Biomial peak fitted ages (P1-P3) were processed by BINOMFIT (Brandon 1996) and given 1σ (95% confidence interval).

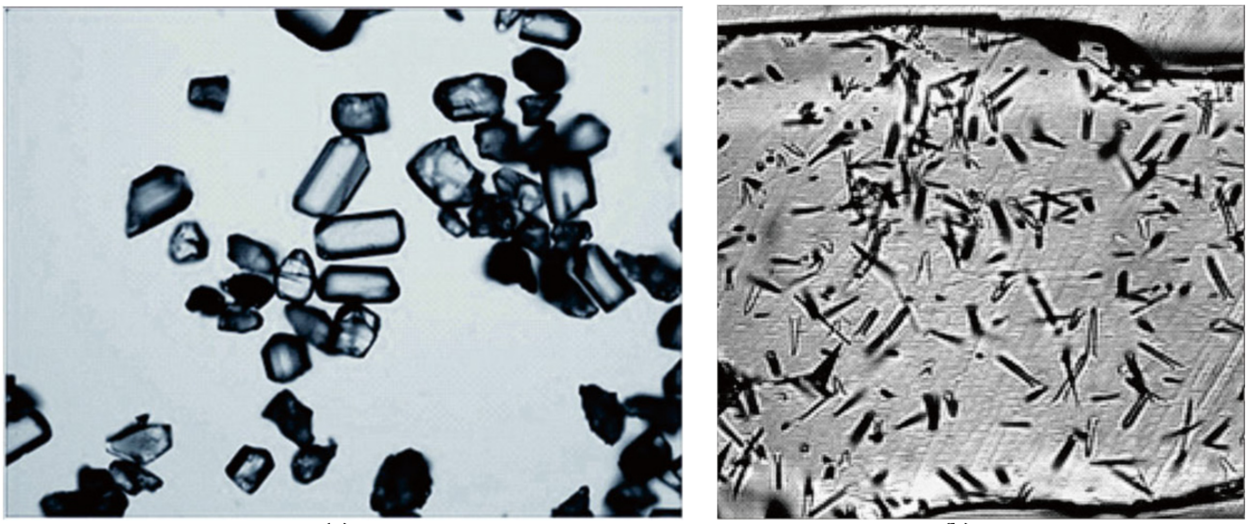

(a) (b)

Figure 4 Apatite grains of different shape (a); etched tracks in one apatite (b).

commonly estimated to be 60°C-110°C±10°C (Green et al. 1985; Hurford 1986).

3 Results

The AFT dating results of six samples are shown in Table 1 and Figure 5. The *P* (x^2) values can evaluate the dated grains as to whether or not they belong to a single age population (Gaabraith and Laslett, 1993). Results from 4 samples (LL1, LL3, LL4 and LL6) passed the x^2 test (>5%), which is used to measure the variation in the single-grain ages (Galbraith and Laslett, 1993). The $P(x^2)$ values of two samples (LL2 and LL5) are below 5%. The pooled ages were reported for those samples which pass the x^2 test, otherwise, the central ages are adopted (Sobel et al. 2006). Radial plot showed samples with a large dispersion of single-grain ages (Figure 5), indicating that samples were mixed with the different source regions (Green 1981). Therefore, it is necessary to analyze single-grain ages for each sample to obtain reliable and meaningful thermo-tectonic information.

All samples were selected from the Lulehe section, dated magnetostratigraphically by Zhang (2006). Thus, the depositional ages were closely constrained. The depositional ages of samples LL1, LL2, LL3, LL4, LL5 and LL6 were 53.41, 51.80, 47.91, 45.93, 41.52 and 38.67 Ma, respectively. AFT central ages, including LL1, LL3, LL4 and LL6, which were 38 Ma, 48 Ma, 46±3 Ma and 65±3 Ma. LL2 and LL5 samples pooled ages were 62±3 and 58±3 Ma. Single-grain ages of apatite from distribution of the Lulehe profile (Table 1) showed that LL1, LL2, LL3 and LL4 single-grain ages with Lulehe Formation were (25.4-95.0 Ma), (23.4-94.6 Ma), (25.0-86.9 Ma) and (18.8-70.15 Ma), respectively. And their youngest age groups were 37.8, 25.1, 43.4 and 45.5 Ma. LL5 single-grain ages with Xiaganchaigou Formation range from 22.4 Ma to 81.5 Ma. The main thermal events occurred at (65-72 Ma), (40-64 Ma) and (32-40 Ma). The lag time was (~4.58 Ma). The minimum age group was (~46.1 Ma). LL6 single-grain ages were between 36.0 Ma and 100.8 Ma. The thermal events took place at ~60, ~68, ~75, ~50, >87 Ma and ~35 Ma, and there was a strong tectonic activity at (44-55 Ma). The lag time was 18.23 Ma. The youngest age population was (~56.9 Ma).

Decomposition of the AFT ages can provide more information. In this paper we used the software (Binom-Fit), which is provided by Brandon (2002). It was used to deal with the AFT dates, and the results are shown in Table 1 and Figure 5. The decomposed fitted peak ages presented for P1, P2 and P3. The peak ages show that P1 ranges from 56.9 Ma to 25.1 Ma for the Lulehe profile. And The P1 peak age represented the youngest age population. The P2 is main peak age, and the age groups are about ~65 Ma. The P3 peak age is less, and only LL2 sample is ~85 Ma.

4 Discussion

4.1 The uplift of the source region at the Late Cretaceous and the Eocene

When one sample is buried to a depth less than the PAZ, the source region formation could be recorded perfectly. Otherwise, the information is progressively erased (Gleadow et al. 2002; van der Beek et al. 2006). Apatites are partially reset or unreset when the AFT age (the central age or the pooled age) is older than the depositional age (Brandon et al. 1998). The youngest AFT ages group could record the uplifting event (Garver et al. 1999; Zheng 2000; van der Beek et al. 2006; Rahl et al. 2007). 5 samples were not annealed or slightly partial annealed as indicated by analyzing LL2, LL3, LL4, LL5 and LL6 due to their AFT ages were older than or equal to the depositional ages. And hence, no annealed samples could save abundance of tectonic information in the source region. Decomposition of the AFT single-grain ages can provide more information. The P1 age groups range from 56.9 Ma to 25.1 Ma. The P2 is main peak age, and the age groups is about 52.0-67.0 Ma. The P3 peak age is less, and only LL2 sample is ~85 Ma. As discussed above, the uplift events divided into the late Cretaceous period (~85 Ma and ~65 Ma) and the Eocene period (~56.9 Ma and 52.0 Ma). The similar uplift events were recorded in the surrounding mountains (Kunlun Shan, Qilian Shan and Altun Shan) of the NQB, all of which have experienced far-field effects of accretion-collision events at the distant continental margins when the Indian Plate collided with the Eurasian Plate (Yin et al. 1998; George et al. 2001; Jolivet et al. 2001;

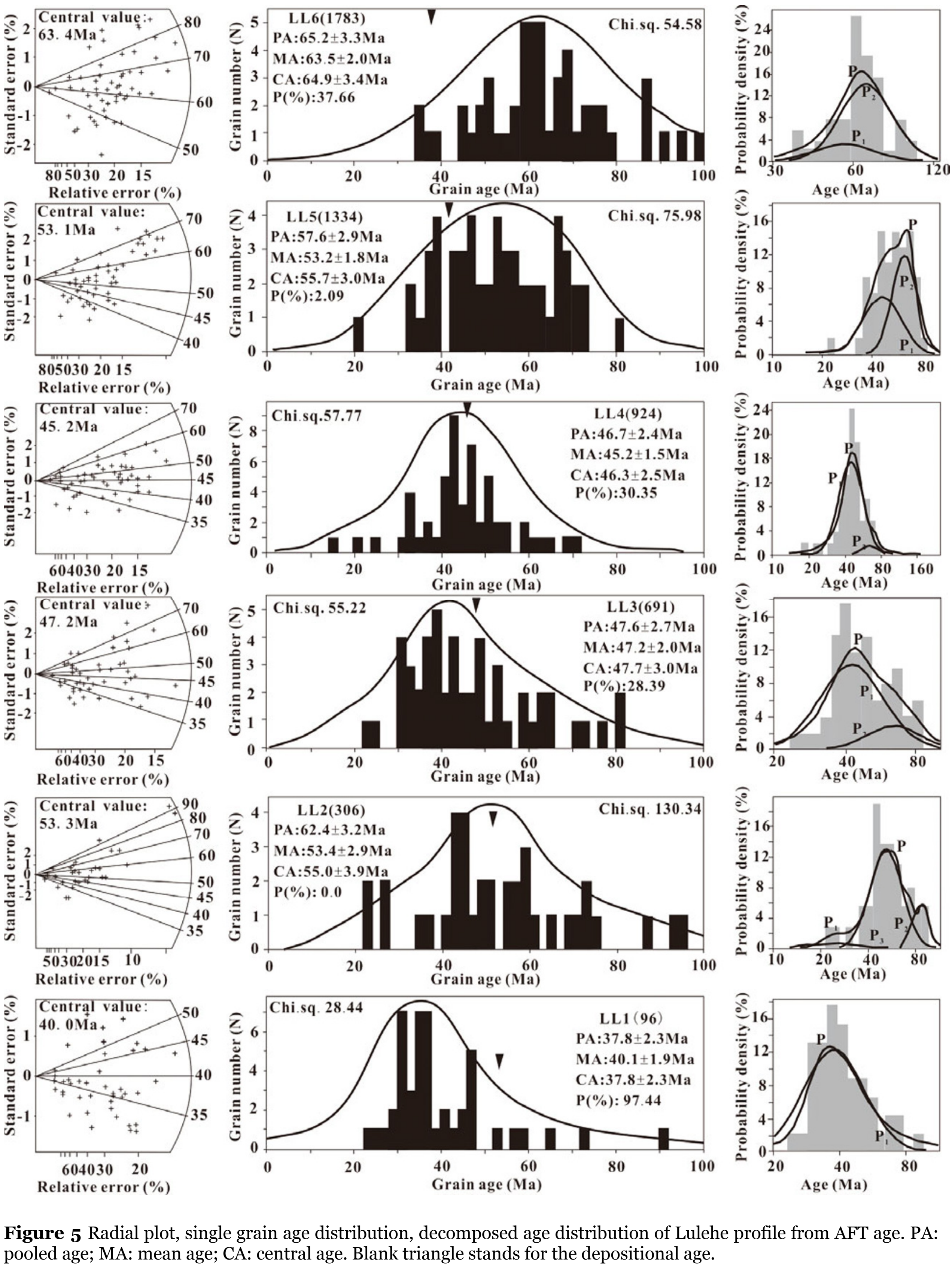

Figure 5 Radial plot, single grain age distribution, decomposed age distribution of Lulehe profile from AFT age. PA: pooled age; MA: mean age; CA: central age. Blank triangle stands for the depositional age.

Wang et al. 2004; Yuan et al. 2006a; Yuan et al. 2006b; Qi et al. 2016). The grains in the basin were sourced from nearby mountains (Sobel and Strecker 2003). The Altun Mountains had been proved on AFT records of the tectonic uplift at (~50 Ma), (~52.9 Ma), (61-24 Ma) and (69.5±2.9 Ma) (Wang et al. 2002; Yin et al. 2002; Chen et al. 2006; Liu 2007; Liu et al. 2012; Lu et al. 2013; Chen et al. 2014); The Kunlun Mountains recorded those AFT ages at (~52.9 Ma), (54-47 Ma), (~67 Ma) and (108-61 Ma) (Bai et al. 2003; Yuan et al. 2006b; Bai et al. 2008; Wang 2010; Chen et al. 2011); Others had been also found in the Qilian Mountains at (49±5 Ma), (60±5 Ma) and (74±10 Ma) (Wang 2010; Wan et al. 2011; Jiang 2011). Jolivet et al. (2001) described the tectonics of the northern edge of the TP by using FT constraints, and the ages were (48±4 Ma), (53±7 Ma) and (96.3-53.8 Ma). As discussed above, it indicates that the main events can be recorded at the late Cretaceous period (~85 Ma and ~65 Ma) and the Eocene period (56.9 Ma and 52.0 Ma) in the NQB.

Thus, the basin recorded the late Cretaceous and the Eocene events for the surrounding mountains of the NQB, all of which have experienced far-field effects of accretion-collision events at the distant continental margins when the Indian Plate collided with the Eurasian Plate.

4.2 The provenance changed at Eocene (~37.8 Ma) and (43.4-46.1 Ma)

Apatites are reset when the AFT age is less than the depositional age (Brandon et al. 1998). LL1 had experienced complete annealing, suggesting that it recorded the strong tectonic activity inside the basin at the Eocene (~37.8 Ma). Similar records were also found with single-grain ages for other samples at (32-40 Ma) in the source region (Figure 5), especially the contents of single-grains are high in the Lulehe profile. Most Eocene deformations were discovered in the Altun Mountains (Jolivet et al. 2001; Wan et al. 2001; Wang et al. 2002). There were also many similar uplift events at Qilian Mountains during the Eocene (Jolivet et al. 2001; Jiang 2011). The sedimentation rate in the Qaidam Basin increased significantly from 0.017 mm/Ma to more than 0.07 mm/Ma after 36.6 Ma due to variation in the rate of slip along the ATF and northeastward-extension of this region (Metivier et al. 1996). Mock et al. (1999) studied on an intense uplifting event at ~30 Ma on the east Kunlun area. Wang et al. (2004) dated the unroofing event of the NQB during the Oligocene-Miocene, and exhibited that this age documented the Cenozoic initial deformation of the NQB. As discussed above, the basin deformation event occurred during the Eocene, which took place almost simultaneously with those in the Altyn Mountains, Kunlun Mountains and Qilian Mountains. Thus, the uplift of North Qaidam range changed the provenance direction at the Eocene (~37.8 Ma).

Apatites are partially reset or unreset when the AFT age is older than the depositional age (Brandon et al. 1998). LL4, LL5 and LL6 samples AFT ages were older than the depositional ages, suggesting that samples were partial reset or unrest. The youngest age population (43.4-46.1 Ma) affirmed that a fast exhumation and cooling event occurred in the source region. In addition, the lag time got short from the top to the bottom in the Lulehe profile, affirming that the exhumation changed fast in the source region at the Palaecene-Eocene (Garver et al. 1999; Zheng 2000; van der Beek et al. 2006; Rahl et al. 2007). And the lag time turned negative from LL1 to LL4 in the Lulehe profile, indicating the provenance changed rapidly due to the deformation of the North Qaidam range at the Palaecene-Eocene significantly. Gao et al. (2009) argued that the north Qaidam thrust belt activity was strong at (~48 Ma). And there was also a strong tectonic activity at (~44 Ma), corresponding to angular unconformity between the Lulehe Formation and Xiaganchaigou Formation (Ren et al. 2004; Yin et al. 2008a; Li et al. 2012; Wang et al. 2017). Norton (1995) studied on plate motions in the Pacific: the 43 Ma non-event. As discussed above, there were a strong tectonic activity at (43.4-46.1 Ma) due to deep burial either related to deposition of a thick Cenozoic sequence or thrusting of a thick hanging-wall section from above at the Eocene (Jolivet et al. 2001; Yin et al. 2008a). Moreover, as shown in the Figure 6, the youngest age groups of LL2 and LL5 are inconsistent with others samples. The difference was related to the Hidden Faults activity. It indicates that the Xiaganchaigou Formation and Lulehe Formation were rapidly uplifted to the surface from ancient APAZ in the late Oligocene.

Therefore, the age population revealed the movement information of the north Qaidam thrust belt at the Eocene. At that time, the basin took place angular unconformity between the Lulehe Formation and Xiaganchaigou Formation due to the early Mesozoic strata tilted and suffered denudation to the thrust fault of the NQB (Jolivet et al. 2001; Yin et al. 2008a).

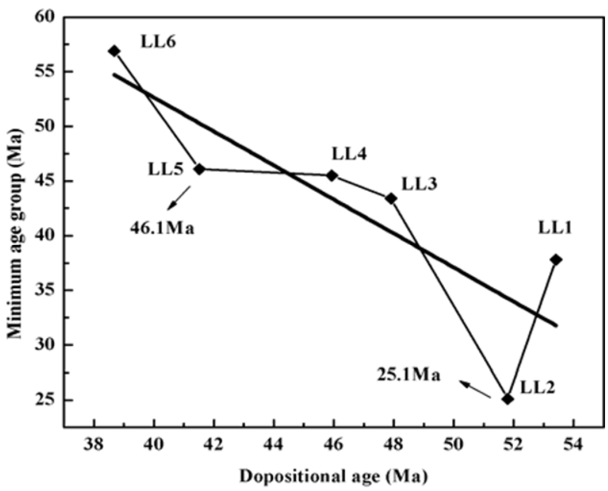

Figure 6 Relationship between the minimum AFT age and the depositional age within Lulehe Profile.

4.3 Provenance analysis

St ratigraphic distribution and lithofacies analysis from the late Paleozoic to the early Mesozoic shows that the area's water retreated from north, west and those around uplifted to the mountains, by which Qaidam Basin was formed (Yin et al. 2008a). Afterwards, it started to form Lake Facies and Lake-river Facies in the Cenozoic.

A considerable amount of various dating works have been done in this region. Altyn Mountains suggested that AFT records of the tectonic uplift event occurred at (5-10 Ma), (7-9 Ma), (9.8-7.2 Ma), (18.1-14.7 Ma), (22-15 Ma), (31-21Ma), (42-11.1 Ma), (~52.9 Ma), (61-24 Ma) and (69.5±2.9 Ma) (Wang et al. 2002; Chen et al. 2006; Liu 2007; Wan et al. 2011; Lu et al. 2013; Chen et al. 2014). Some studies that focused on the Kunlun Mountains indicated that AFT ages were at (5.1-0.9 Ma), (6.3-10 Ma), (15.8±1.1 Ma), (22-16.5 Ma), (26.6-17.8 Ma), (~52.9 Ma), (54-47 Ma), (~67 Ma), (108-61 Ma) and (120-100 Ma) (Bai et al. 2003; Yuan et al. 2006b; Bai et al. 2008; Wang 2010; Chen et al. 2011); others had also worked on AFT thermochronology in the Qilian Mountains proposed that the uplifting events were at (13±2 Ma), (26.6-17.8 Ma), (32.5-16.2 Ma), (32±4 Ma), (49±5 Ma), (60±5 Ma), (74±10 Ma), (88±11 Ma), (89±9 Ma), (93±7 Ma), (93±10 Ma), (96±8 Ma), (96.3-53.8 Ma), (98±8 Ma), (103±13 Ma), (108-61 Ma), (112±21 Ma), (114±8 Ma), (114±9 Ma) and (124±11 Ma) (Wan et al. 2011; Jiang 2011; Qi et al. 2016). Jolivet et al. (2001) had described tectonics of the northern edge of the TP by using FT constraints, and the ages were at (10±1 Ma), (17±2 Ma), (18±1 Ma), (19±2 Ma), (21±2 Ma), (30±4 Ma), (32.5-16.2 Ma), (48±4 Ma), (53±7 Ma), (96.3-53.8 Ma), (105±5 Ma), (127±7 Ma), (134±5 Ma), (134±10 Ma), (138±8 Ma) and (147±10 Ma), respectively. AFT statistic results showed in the Altun, East Kunlun and Qilian Mountains were all found in the surrounding area of the Qaidam Basin (Figure 7), the study area recorded the uplift event in the Late Cretaceous (~65 Ma, ~68 Ma, ~73 Ma, ~75 Ma, ~81.5 Ma, ~86.9 Ma, ~87 Ma, ~94.6 Ma, ~95.0 Ma and ~100.8 Ma) and (65-70.2 Ma), the Eocene (~53 Ma) and (43.4-46.1 Ma), and it revealed that the sediments were mainly derived from the north mountains (Green spot in Figure 7). The grains in the basin were sourced from nearby mountains or highlands (Sobel and Strecker 2003). Yin et al. (2008a and b) reported the north and south parts of the Qaidam basin were primarily controlled by the north Qaidam thrust belt, and the Lulehe section provenance was mainly derived from the north mountains or highlands in surrounding area of the NQB by paleocurrent analysis in the Cenozoic. Lu et al. (2014) suggested foreland uplift provenance was mainly derived from sediment within the north Qaidam thrust belt during (34-8.5 Ma) in the Dahonggou section (Figure 8). Considering the single-grain ages of the source region, sediments were mainly derived from the south Qilian Shan and Altun Shan. Based on analysis of heavy minerals, paleocurrent and clastic particles grading, the south Qilian and ATF orogenic belts are the main provenance for the NQB (Rieser et al. 2005; Li et al. 2009; Fu et al. 2013; Lin et al. 2014; Li et al. 2014; Li et al. 2015; Peng et al. 2015). The conclusion was consistent with the analysis result obtained by the previous scholars. Thus, these piedmont faults (ATF and

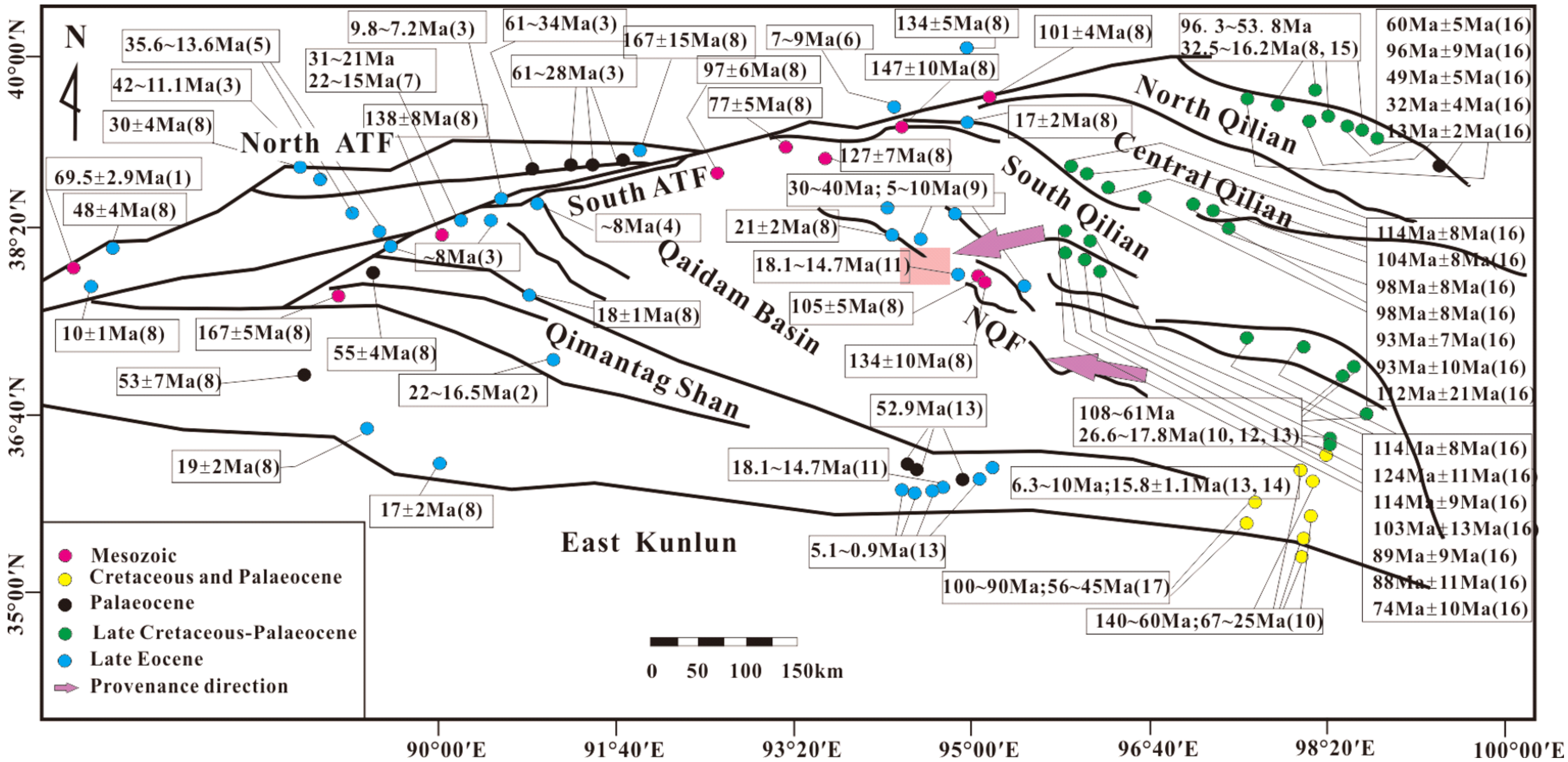

Figure 7 Distribution of AFT ages of the surrounding mountains in the Qaidam Basin. 1: Kunlun Mountains (Bai et al. 2003); 2: Qimantag Mountains (Bai et al. 2008); 3: Altun Mountains (Chen et al. 2006); 4: Altun Mountains (Chen 2002); 5: Altun Mountains (Chen et al. 2001); 6: Northern Althn (Wan 2001); 7: Altyn Tagh Fault (Wang et al. 2002); 8: Northern Edge of the Tibetan Plateau (Jolivet et al. 2001); 9: Saishiteng shan (Wan et al. 2011); 10: Eastern Kunlun Mountains (Yuan et al. 2006b); 11: Around Qaidam Basin (Wang et al. 2004); 12: Elashan Range (Lu et al. 2013); 13: East Kunlun Mountains (Chen et al. 2011); 14: Eastern Kunlun Orogen (Wang 2010); 15: Northern Qilian Mountains (Jiang 2011); 16: Eastern Kunlun (Wang 2010); 17: Qilian Mountains (Qi et al. 2016). Arrow line is

north Qaidam thrust belt) not only control the development of Qaidam Basin, but also the result in the uplifting-denudation for strike-slip and reverse movement around the mountain. It also provided abundance of provenance for the basin deposits (Huang et al. 1989; Zhuang et al. 2011b).

As discussed above, based on the new dating evidences, the development of the NQB can be reconstructed approximately in Figure 9. Present configuration of the NQB shown as Figure 9A. The Dasaibei, Xiaosaibei, and Qaidam Shan thrusts zone started to develop, and were associated with deposition of the Lulehe Formation during the Paleocene and early Eocene (Figure 9B). Sediments

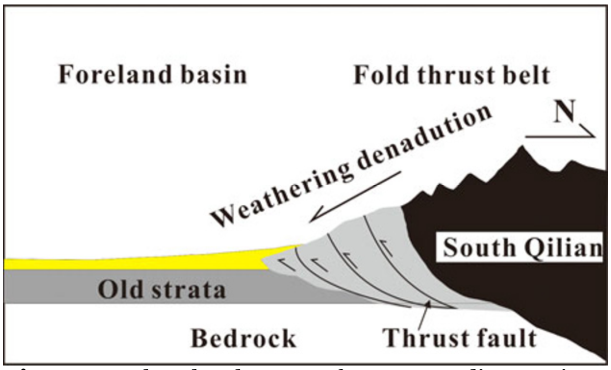

Figure 8 The sketch map of tectono-sedimentation regime in the Northern Qaidam Basin (modified from Lu et al. 2014).

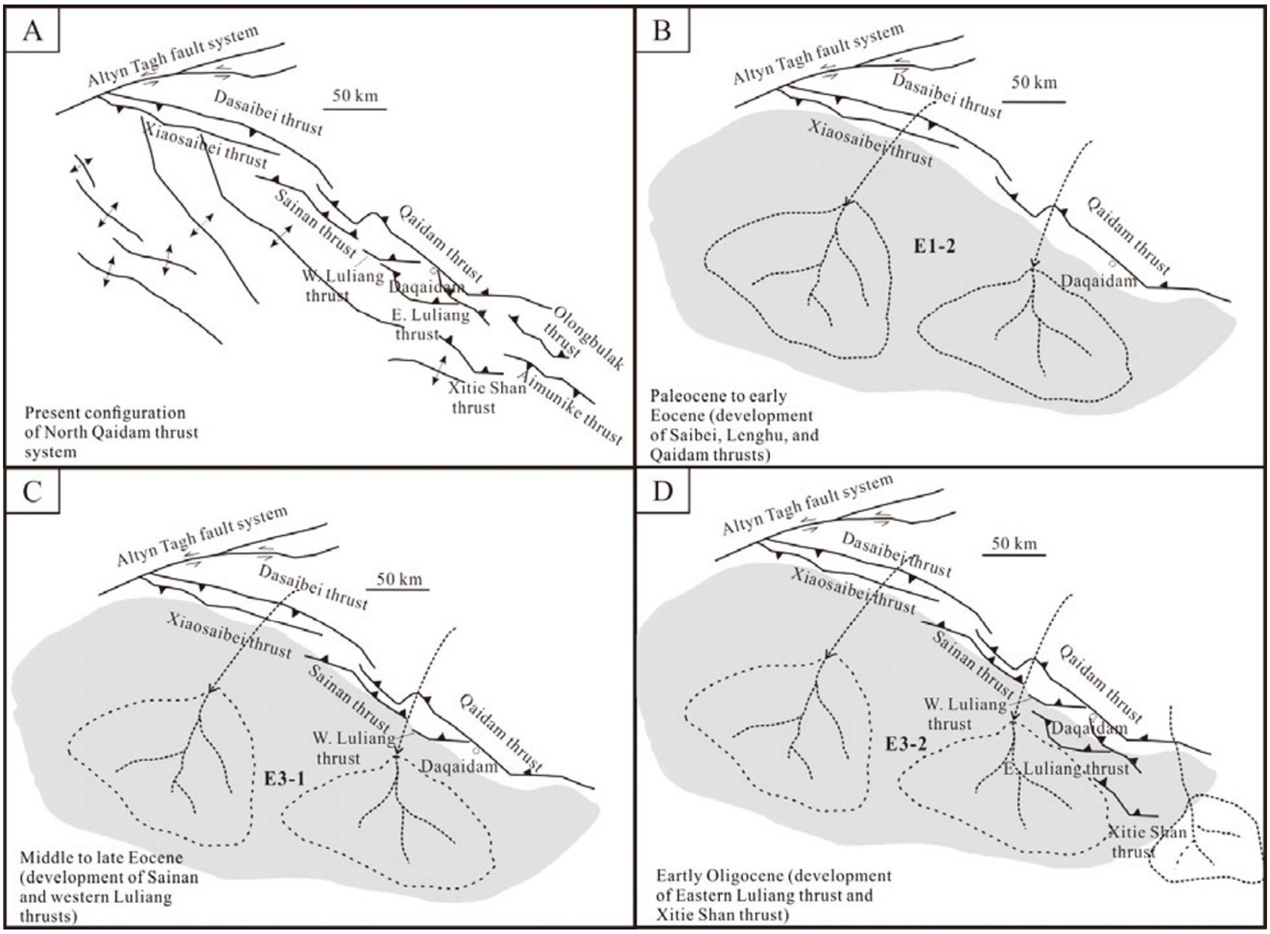

Figure 9 Tectonic evolution of the North Qaidam thrust system and depositional history of the Northern Qaidam Basin. (A) Present tectonic configuration of the North Qaidam thrust belt. (B) The Paleocene-early Eocene tectonic configuration of North Qaidam. (C) The Middle to late Eocene tectonic configuration of North Qaidam. (D) The Early Oligocene tectonic configuration of North Qaidam (Yin et al. 2008a).

were mainly derived from the south Qilian and Altun Shan. The Sainan and the western Luliang Shan thrusts were initiated, and were associated with deposition of the lower Xiaganchaigou Formation in the middle to late Eocene, (Figure 9C). Foreland uplift provenance was mainly derived from sediment within the north Qaidam thrust belt. The Eastern Luliang and Xitie Shan thrusts developing the upper Xiaganchaigou Formation was deposited in the early Oligocene (Yin et al. 2008a and b), (Figure 9D). Foreland uplift provenance was mainly derived from sediment within the north Qaidam thrust belt and south Qilian Shan.

5 Conclusions

The following conclusions are drawn on the basis of the present study:

(1) The study of detrital AFT dates showed that the source region had experienced the main cooling and uplifting processes in the Late Cretaceous period (~87 Ma and ~65 Ma) and the Eocene (~53 Ma), which indicated the northeastern Tibet Plateau characterized by multi-stage and synchronous uplifting before the Cenozoic.

(2) The AFT data revealed the deformation of the North Qaidam thrust belt generated to the provenance change at the Eocene (~37.8 Ma) and (43.4-46.1 Ma) in the Lulehe district.

(3) The present study also suggested that the provenance for sediments of the Lulehe area was derived from the south Qilian Shan and Altun Shan.

Acknowledgements

The authors are very grateful to anonymous reviewer and editor for suggesting necessary valuable corrections in the manuscript. The research reported in this manuscript is funded by the Natural Science Foundation of China (Grants No. 41501209 and 41571177) and the Fundamental Research Funds for the Central Universities (862457, lzujbky-2016-22).

References

Anczkiewicz AA, Środoń J, Zattin M (2013) Thermal history of the Podhale Basin in the internal Western Carpathians from the perspective of apatite fission track analyses. Geologica Carpathica 64: 141-151. https://doi.org/10.2478/geoca-2013-0010

Bai DY, Meng DB, Liu YR, et al. (2003) Apatite fission-track records of the tectonic uplift of the central segment fo the Kunlun Mountains on the northern margin of the Qinghai-Tibet Plateau. Chinese Geology 30: 240-246. https://doi.org/10.3969/j.issn.1000-3657.2003.03.003 (In Chinese)

Bai YS, Ren EF, Fan GL, et al. (2008) Apatite fission track evidence for the Miocene rapid uplift of the Qimantag Mountains on the northwestern margin of the Qinghai-Tibet Plateau. Geological Bulletin of China 27: 1044-1048. https://doi.org/10.3969/j.issn.1671-2552.2008.07.015 (In Chinese)

Brandon MT (2002) Decomposition of mixed grain age distributions using Binomfit. On Track 24: 13-18.

Brandon MT (1996) Probability density plot for fission-track grain-age samples. Radiat. Meas 26(5): 663-676. https://doi.org/10.1016/S1350-4487(97)82880-6

Brandon MT, Rodentice MK, Garver JI (1998) Late Cenozoic exhumation of the Cascadia accretionary wedge in the Olympic mountains, northwest Washington State. Wiley Interdisciplinary Reviews Rna 4: 617-630. https://doi.org/10.1130/0016-7606 (1998)110<0985:lceotc>2.3.co;2

Cande SC, Kent DV (1995) Revised calibration of geomagnetic polarity time scale for the Late Cretaceous and Cenozoic. Journal of Geophysical Research Solid Earth 100: 6093-6095. http:// doi.org /10.1029/94JB03098

Carlson WD, Donelick RA, Ketcham RA (1999) Variability of apatite fission-track annealing kinetics: I. experimental results. American Mineralogist 84: 1213-1223. https://doi.org/10.2138/am-1999-0901

Chen B, Chen F, Wu Z, et al. (2015) Diagenesis and favorable diagenetic facies of Paleogene Lulehe formation sandstone in Lenghu region. Geological Science & Technology Information 34(4): 20-27. (In Chinese)

Chen J, Shi J, Long GH, et al. (2013) Sedimentary facies and models for the Palaeogene-Neogene deposits on the northern margin of the Qaidam basin, Qinghai. Sedimentary Geology & Tethyan Geology 33(3): 16-26. (In Chinese)

Chen K, Bowler JM (1986) Late Pleistocene evolution of salt lakes in the Qaidam basin, Qinghai Province, China. Palaeogeograph. Palaeoclimatal. Palaeoecol 54: 87-104. https://doi.org/10.1016/ 0031-0182(86)90119-7

Chen X, Yuan W, Zhang A, et al. (2014) Apatite fission track analysis for revealing tectonic events of the Bayinguole area in the west section of eastern Kunlun Mountains, northern Qinghai-Tibet Plateau. Nuclear Techniques 37(1): 54-61. (In Chinese)

Chen XH, Wmcrivette M, Li LI, et al. (2011) Thermochronological evidence for multi-phase upliftingof the east Kunlun Mountains, northern Tibetan Plateau. Geological Bulletin of China 30: 1647-1660. https://doi.org/10.3969/j.issn.1671-2552.2011.11.001 (In Chinese)

Chen Z, Washburn Z (2001) Fission track dating of apatite constrains on the Cenozoic uplift of the Altyn Tagh Mountain. Acta Geosicientia Sinica 22(5): 413-418.

Chen ZL, Gong HL, Li L, et al. (2006) Cenozoic uplifting and exhumation process of the Altyn Tagh mountains. Earth Science Frontiers 13: 91-102. https://doi.org/10.3321/j.issn:1005-2321. 2006.04.008

Chen ZW, Wang JL, Wang XF, et al. (2002) Rapid strike-slip of the Altyn Tagh Fault at 8 Ma and its geological implications. Acta Geosicientia Sinica 23: 295-300.

Cheng F, Jolivet M, Fu S, et al. (2016) Large-scale displacement along the Altyn Tagh fault (north Tibet) since its Eocene initiation: insight from detrital zircon U–Pb geochronology and subsurface data. Tectonophysics 677-678: 261-279. https://doi.org/10.1016/ j.tecto.2016.04.023

Crowley KD, Cameron M, Schaefer RL (1991) Experimental studies of annealing of etched fission tracks in fluorapatite. Geochimica Et Cosmochimica Acta 55: 1449-1465. https://doi.org/10.1016/0016-7037(91)90320-5

Danišík M, Kohút M, Broska I, et al. (2010) Thermal evolution of the Malá Fatra mountains (Central Western Carpathians): insights from zircon and apatite fission track thermochronology. Geologica Carpathica 61: 19-27. https://doi.org/10.3321/j.issn:1005-2321.2006.04.008

Emmel B, Geiger M, Jacobs J (2006) Detrital apatite fission-track ages in Middle Jurassic strata at the rifted margin of W Madagascar—indicator for a protracted resedimentation history. Sedimentary Geology 186: 27-38. https://doi.org /10.1016/j.sedgeo. 2005.09.022

Fang X, Zhang W, Meng Q, et al. (2007) High-resolution magnetostratigraphy of the Neogene Huaitoutala section in the eastern Qaidam Basin on the NE Tibetan Plateau, Qinghai Province, China and its implication on tectonic uplift of the NE Tibetan Plateau. Earth & Planetary Science Letters 258, 293-306. https://doi.org/10.1016/j.epsl.2007.03.042

Foster GL, Carter A (2007) Insights into the patterns and locations of erosion in the Himalaya — a combined fission-track and in situ Sm–Nd isotopic study of detrital apatite. Earth and Planetary Science Letters 257: 407-418. https://doi.org/10.1016/j.epsl.2007. 02.044

Fu L, Ping G, Zhao WY, et al. (2013) Heavy mineral feature and provenance analysis of Paleogene Lulehe Formation in Qaidam Basin. Acta Petrologica Sinica 29: 2867-2875.

Gallagher K, Brown R, Johnson C (1998) Fission track analysis and its applications to geological problems. Annual Review of Earth & Planetary Sciences 26: 519-572. https://doi.org/10.1146/annurev. earth.26.1.519

Galbraith RF, Laslett GM (1993) Statistical models for mixed fission track ages. Nucl. Tracks Radiat. Meas 21 (4): 459-470. https://doi.org/10.1016/1359-0189(93)90185-C

Gao JP, Peng YH, Song CH, et al. (2009) Constraints of Cenozoic detrial zircon fission-track age to exhumation-provenance in Qaidam Basin. Global Geology 28: 148-156. https://doi.org/10.3969/j.issn.1004-5589.2009.02.002 (In Chinese)

Garver JI, Brandon MT, Rodentice M, et al. (1999) Exhumation history of orogenic highlands determined by detrital fission-track thermochronology. Geological Society London Special Publications 154: 283-304. https://doi.org/10.1144/gsl.sp.1999.154.01.13

George AD, Marshallsea SJ, Wyrwoll KH, et al. (2001) Miocene cooling in the northern Qilian Shan, northeastern margin of the Tibetan Plateau, revealed by apatite fission-track and vitrinite-reflectance analysis. Geology 29: 939. https://doi.org/10.1130/0091-7613(2001)029<0939:mcitnq>2.0.co;2

Gleadow AJW, Belton DX, Kohn BP, et al. (2002) Fission track dating of phosphate minerals and the chermochronology of apitite. Rev. Mineral. Geochem 48(1): 579-630. https://doi.org/10.2138/rmg.2002.48.16

Green PF (1981) A new look at statistics in fission-track dating. Nuclear Tracks 5: 77-86. https://doi.org/10.1016/0191-278X(81)90029-9

Green PF, Crowhurst PV, Duddy IR, et al. (2006) Conflicting (U–Th)/He and fission track ages in apatite: enhanced He retention, not anomalous annealing behaviour. Earth & Planetary Science Letters 250: 407-427. https://doi.org/10.1016/j.epsl.2006.08.022

Green PF, Duddy IR, Gleadow AJW, et al. (1985) Fission-track annealing in apatite: track length measurements and the form of the Arrhenius plot. Nuclear Tracks & Radiation Measurements 10: 323-328. https://doi.org/10.1016/0735-245x(85)90121-8

Huang H, Zhou X, Wang C (1989) Tectonic evolution of the Qaidam basin and the regularity of oil accumulation. Geological Review 55: 314-323. (In Chinese)

Hurford AJ (1986) Cooling and uplift patterns in the Lepontine Alps South Central Switzerland and an age of vertical movement on the Insubric fault line. Contributions to Mineralogy & Petrology 92: 413-427. https://doi.org/10.1007/ bf00374424

Hurford AJ, Green PF (1982) A users' guide to fission track dating calibration. Earth and Planetary Science Letters 59: 343-354. http://doi.org/10.1016/0012-821x(82)90136-4

Hurford AJ, Green PF (1983) The Zeta age calibration of fission track dating. Chemical Geology (Isotope Geoscience Section) 1: 285-317. https://doi.org/10.1016/S0009-2541(83)80026-6

Jiang SF (2011) Study on apatite fission-track thermochronology in northern Qilian Mountain. PhD thesis, Lanzhou University 5-6. (In Chinese)

Jolivet M, Brunel M, Seward D, et al. (2001) Mesozoic and Cenozoic tectonics of the northern edge of the Tibetan plateau: fission-track constraints. Tectonophysics 343: 111-134. https://doi.org/10.1016/s0040-1951(01)00196-2

Li FJ, Li JW, Wang HF, et al. (2014) The heavy minerals characteristics and provenance analysis of the Neogene in north margin of Qaidam Basin. Science Technology & Engineering 17: 182-187. https://doi.org /10.3969/j.issn.1671-1815.2014.17.036 (In Chinese)

Li FJ, Liu Q, Liu DH, et al. (2009) Characteristics and influential factors of low-Ganchaigou Formation reservoir in north edge of Qaidam Basin. Natural Gas Geoscience 20: 44-49. (In Chinese)

Li JW, Yang C, Li F, et al. (2015a) Provenance analysis of the Neogene in Eboliang area, Qaidam Basin. Journal of Palaeogeography 17(2): 186-197. (In Chinese)

Li JW, Yang C, Li FJ, et al. (2015b) Provenance analysis of the Paleoogene in Eboliang area,Qaidam basin. Acta Sedimentological Sinica 33(4): 649-658. (In Chinese)

Li LL, Guo ZJ, Guan SW, et al. (2015) Heavy mineral assemblage characteristics and the Cenozoic paleogeographic evolution in southwestern Qaidam Basin. China Science: Earth Science 58: 859-875.

Li MY, Yue XA, Jiang QC, et al. (2012) Relationship between hydrocarbon accumulation and tectonic evolution in main structural belt of the northern border of Qaidam Basin. Natural Gas Geoscience 23: 461-468. (In Chinese)

Lin H, Li Fj, Li Lei, et al. (2014) Characteristics of Paleogene heavy mineral and its source in Northern margin of Qaidam Basin. Natural Gas Geoscience 25: 532-541. (In Chinese)

Li FJ, Li JW, Wang HF, et al. (2014) The heavy minerals characteristics and provenance analysis of the Neogene in north margin of Qaidam basin. Science Technology & Engineering 14(17): 182-187. (In Chinese)

Lin X, Zheng D, Sun J, et al. (2016) Detrital apatite fission track evidence for provenance change in the Subei Basin and implications for the tectonic uplift of the Danghe Nan Shan(NW China) since the mid-Miocene, Institute of Geology and Geophysics, Chinese Academy of Sciences. pp. 302-311.

Liu C, Ma YS, Zhou JJ, et al. (2012) Evidence for the Carboniferous hydrocarbon generation in Qaidam Basin. Acta Petrolei Sinica 33: 925-931.

Liu Y (2007) Geochronology of the Altun Fault zone and rising of the Altun Mountains. Chinese Journal of Geology. 42 (1): 134-146. https://doi.org/10.3321/j.issn:0563-5020.2007.01.012

Liu Y, Genser J, Ge X, et al. (2003) $^{40}Ar/^{39}Ar$ age evidence for Altyn fault tectonic activities in western China. Chinese Science Bulletin 48: 2024-2030.

Lu H, Wang E, Shi X, et al. (2013) Cenozoic tectonic evolution of the Elashan range and its surroundings, northern Tibetan Plateau as constrained by paleomagnetism and apatite fission track analyses. Institute of Geology and Geophysics, Chinese Academy of Sciences. pp 150-161.

Lu H, Wang E & Meng K (2014) The mid-miocene tectonic uplift of southern qilianshan: sedimentary evidence from dahonggou section in qaidam basin. Chinese Journal of Geology 49(1), 95-103. https://doi.org /10.3969/j.issn.0563-

5020.2014.01.007
Lu H, Xiong S (2009) Magnetostratigraphy of the Dahonggou section, northern Qaidam Basin and its bearing on Cenozoic tectonic evolution of the Qilian Shan and Altyn Tagh Fault. Earth & Planetary Science Letters 288: 539-550. https://doi.org/10.1016/j.epsl.2009.10.016
Metivier F, Ccedil ois (1996) Volumes sédimentaires et bilans de masses en Asie pendant le Cénozoïque, Que. PhD thesis, Univ. Paris 7.
Mock C, Arnaud NO, Cantagrel JM (1999) An early unroofing in northeastern Tibet? Constraints from 40 Ar/ 39 Ar thermochronology on granitoids from the eastern Kunlun range (Qianghai, NW China). Earth & Planetary Science Letters 17: 107-122. https://doi.org/10.1016/s0012-821x(99)00133-8
Naeser CW (1979) Fission-track dating and geologic annealing of fission tracks. Springer Berlin Heidelberg. pp 154-169. https://doi.org/10.1007/978-3-642-67161-6_10
Naylor M, Sinclair HD, Bernet M, et al. (2015) Bias in detrital fission track grain-age populations: Implications for reconstructing changing erosion rates. Earth & Planetary Science Letters 422: 94-104. https://doi.org/10.1016/j.epsl.2015.04.020
Norton IO (1995) Plate motions in the North Pacific: The 43 Ma nonevent. Tectonics 14: 1080-1094. https://doi.org/10.1029/95tc01256
Oliveira CHED, Jelinek AR, Jr FC, et al. (2016) Thermotectonic history of the southeastern Brazilian margin: Evidence from apatite fission track data of the offshore Santos Basin and continental basement. Tectonophysics 685: 21-34. https://doi.org/10.1016/j.tecto.2016.07.012
Olivetti V, Balestrieri ML, Rossetti F, et al. (2013) Tectonic and climatic signals from apatite detrital fission track analysis of the Cape Roberts Project core records, South Victoria Land, Antarctica. Tectonophysics 594: 80-90. https://doi.org/10.1016/j.tecto.2013.03.017
Peng Y, Sheng MY, Lin LC, et al. (2015) An analysis of late Hercynian–Indosinian Paleotectonic stress on the northern margin of the Qaidam Basin. Acta Geoscientica Sinica 36: 51-59. https://doi.org /10.3975/cagsb.2015.01.06
Qi B, Hu D, Yang X, et al. (2016) Apatite fission track evidence for the Cretaceous–Cenozoic cooling history of the Qilian Shan (NW China) and for stepwise northeastward growth of the northeastern Tibetan Plateau since early Eocene. Journal of Asian Earth Sciences 124: 28-41. https://doi.org/10.1016/j.jseaes.2016.04.009
Rahl JM, Ehlers TA, Pluijm BAvd (2007) Quantifying transient erosion of orogens with detrital thermochronology from syntectonic basin deposits. Earth and Planetary Science Letters 256: 147-161. https://doi.org/10.1016/j.epsl.2007.01.020
Ren S, Ge XH, Liu Y, et al. (2004) Multi-stage strike-slip motion and uplift along the Altyn Tagh fault since the Late Cretaceous. Regional Geology of China 23: 926-932.
Rieser AB, Neubauer F, Liu Y, et al. (2005) Sandstone provenance of north-western sectors of the intracontinental Cenozoic Qaidam basin, western China: Tectonic vs. climatic control. Sedimentary Geology 177: 1-18. https://doi.org/10.1016/j.sedgeo.2005.01.012
Ritts BD, Yue YJ, Graham, SA (2004) Oligocene-Miocene tectonics and sedimentation along the Altyn Tagh Fault, Northern Tibetan Plateau: analysis of the Xorkol, Subei, and Aksay Basins. Journal of Geology 112: 207-229. https://doi.org/10.1086/381658
Roger F, Jolivet M, Malavieille J (2010) The tectonic evolution of the Songpan-Garzê (North Tibet) and adjacent areas from Proterozoic to present: a synthesis. Journal of Asian Earth Sciences 39: 254-269. https://doi.org/10.1016/j.jseaes.2010.03.008
Sobel ER, Strecker MR (2003) Uplift, exhumation and precipitation: tectonic and climatic control of Late Cenozoic landscape evolution in the northern Sierras Pampeanas, Argentina. Basin Research 15: 431–451. https://doi.org/10.1046/j.1365-2117.2003.00214.x
Sobel ER, Chen J, Heermance RV (2006) Late Oligocene-Early Miocene initiation of shortening in the southwestern Chinese Tian Shan: implications for Neogene shortening rate aruations. Earth and Planetary Science Letters 247 (1-2), 70-81. https://doi.org/10.1016/j.epsl. 2006.03.048
Sun J, Zhu R, An Z (2005) Tectonic uplift in the northern Tibetan Plateau since 13.7 Ma ago inferred from molasse deposits along the Altyn Tagh Fault. Earth & Planetary Science Letters 235, 641-653. https://doi.org/10.1016/j.epsl.2005.04.034
Sun GQ, Du ZM, Ji YY, et al. (2012) Sedimentary model since Paleogene in northern margin of Qaidam basin. Lithologic Reservoirs 24(4): 13-18. (In Chinese)
Sun GQ, Chen B, Zheng Y, et al. (2015) Diagenesis and sedimentary environment of miocene in lenghu Ⅴ tectonic belt. Natural Gas Geoscience. 26 (4): 679-688. https://doi.org/10.11764/j.issn.1672-1926.2015.04.0679 (In Chinese)
van der Beek P, Robert X, Mugnier JL, et al. (2006) Late Miocene – Recent exhumation of the central Himalaya and recycling in the foreland basin assessed by apatite fission - track thermochronology of Siwalik sediments, Nepal. Basin Research 18: 413-434. https://doi.org/10.1111/j.1365-2117.2006.00305.x
Wan JL (2011). Modeling Thermal history during low temperature by K-feldspar MDD and fission track: example from Meso-Cenozoic tectonic evolution in Saishitengshan in the northern Margin of Qaidam Basin. Seismology & Geology 33: 369-382. https://doi.org/10.3969/j.issn.0253-4967.2011.02.010 (In Chinese)
Wan JL, Wang Y, Li Q, et al. (2001) Fission track evidence of Northern Altyn uplift in late-Cenozoic. Bulletin of Mineralogy Petrology & Geochemistry 20: 222-224. https://doi.org/10.3969/j.issn.1007-2802.2001.04.004 (In Chinese)
Wang A,Wang GC, Zhang KX (2010) An early Cenozoic tectonic event in eastern Kunlun orogen, evidence from detrital fission track geochronology, evidence from detrital fission track geochrnology. Earth Science: Journal of China University of Geosciences 35: 737-746. https://doi.org/10.3799/dqkx.2010.088
Wang B, Liu CL, Li ZX, et al. (2017) Tectonic-stress field and tectonic evolution in the eastern Qaidam basin since Mesozoic. Journal of Earth Sciences & Environment 39: 83-94.
Wang E (1997) Displacement and timing along the northern strand of the Altyn Tagh fault zone, Northern Tibet. Earth and Planetary Science Letters 150: 55-64. https://doi.org/10.1016/ s0012-821x(97)00085-x
Wang F, Lo CH, Li Q, et al. (2004) Onset timing of significant unroofing around Qaidam basin, northern Tibet, China: constraints from Ar/Ar and FT thermochronology on granitoids. Journal of Asian Earth Sciences 24: 59-69. https://doi.org/ 10.1016/j.jseaes.2003.07.004
Wang X, Song C, Zattin M, et al. (2016) Cenozoic pulsed deformation history of northeastern Tibetan Plateau reconstructed from fission-track thermochronology. Tectonophysics 672-673: 212-227. https://doi.org/10.1016/j.tecto.2016.02.006
Wang Y, Wan J, Li Q, et al. (2002) Fission-track evidence for the Cenozoic uplift and erosion of the northern segment of the Altyn Tagh fault zone at the Aksay-Dangjin Pass. Acta Geologica Sinica 76: 191-198.
Wei GQ, Li BL, Xiao AC, et al. (2005) Strike-thrust structures and petroleum exploration in northern Qaidam Basin. Earth Science Frontiers 12: 397-402. https://doi.org/10.3321/j.issn:1005-2321. 2005. 04.008
Wendt AS, Vidal O, Chadderton LT (2002) Experimental evidence for the pressure dependence of fission track annealing in apatite. Earth & Planetary Science Letters 201: 593-607. https://doi.org/10.1016/s0012-821x(02)00727-6
Yang W, Jolivet M, Dupont-Nivet G, et al. (2014) Mesozoic-Cenozoic tectonic evolution of southwestern Tian Shan:

evidence from detrital zircon U/Pb and apatite fission track ages of the Ulugqat area, Northwest China. Gondwana Research 26: 986-1008. https://doi.org/10.1016/j.gr.2013.07.020
Yin A, Dang YQ, Wang LC, et al. (2008a) Cenozoic tectonic evolution of Qaidam basin and its surrounding regions (Part 1): The southern Qilian Shan-Nan Shan thrust belt and northern Qaidam basin. Geological Society of America Bulletin 120: 813-846. https://doi.org/10.1130/b26180.1
Yin A, Dang YQ, Zhang M, et al. (2008b) Cenozoic tectonic evolution of Qaidam Basin and its surrounding regions (Part 3): Structural geology, sedimentation, and regional tectonic reconstruction. Geological Society of America Bulletin 120 (7-8): 847-876. https://doi.org/10.1130/B26232.1.
Yin A, Nie S, Craig P, et al. (1998) Late Cenozoic tectonic evolution of the southern Chinese Tian Shan. Tectonics 17: 1-27. https://doi.org/10.1029/97tc03140
Yin A, Rumelhart PE, Butler R, et al. (2002) Tectonic history of the Altyn Tagh fault system in northern Tibet inferred from Cenozoic sedimentation. Geological Society of America bulletin 114: 1257-1295. https://doi.org/10.1130/0016-7606(2002)114<1257:thotat> 2.0.co;2
Yuan W, Carter A, Dong J, et al. (2006a) Mesozoic–Tertiary exhumation history of the Altai Mountains, northern Xinjiang, China: New constraints from apatite fission track data. Tectonophysics 412: 183-193. https://doi.org/10.1016/j.tecto.2005.09.007
Yuan WM, Dong J, Wang S, et al. (2006b) Apatite fission track evidence for Neogene uplift in the eastern Kunlun Mountains, northern Qinghai-Tibet Plateau, China. Journal of Asian Earth Sciences 27: 847-856. https://doi.org/10.1016/j.jseaes.2005.09.002
Yuan WM, Bao ZK, Dong JQ (2007). Fission track analysis of metallogenic age of Tuwu-Yandong porphyre copper deposit and tectonic motion in Xingjiang. Science in China 37: 1330-1337.
Zhang J, Wang YN, Zhang BH, et al. (2015) Evolution of the NE Qinghai–Tibetan Plateau, constrained by the apatite fission track ages of the mountain ranges around the Xining Basin in NW China. Journal of Asian Earth Sciences 97: 10-23. https://doi.org/10.1016/j.jseaes.2014.10.002
Zhang PZ, Peter M, et al. (2001). Increased sedimentation rates and grain sizes 2-4 Myr ago due to the influence of climate change on erosion rates. Nature 410: 891-897. https://doi.org/10.1038/35073504
Zhang WL (2006) Cenozoic uplift of the Tibetan Plateau: evidence from high resolution magnetostratigraphy of the Qaidam Basin. PhD thesis, Lanzhou University. pp 95-105. (In Chinese)
Zhang ZY, Zhu WB, Shu LS, et al. (2009) Apatite fission track thermochronology of the Precambrian Aksu blueschist, NW China: Implications for thermo–tectonic evolution of the north Tarim basement. Gondwana Research 16: 182-188. https://doi.org/10.1016/j.gr.2009.04.006
Zheng D (2000) Detrital grain thermochronology-a potential method for research on coupling process between Basin and Mountain. Seismology & Geology 22(S): 25-36. (In Chinese)
Zheng DW, Clark MK, Zhang PZ, et al. (2010) Erosion, fault initiation and topographic growth of the North Qilian Shan (northern Tibetan Plateau). Geosphere 6: 937-941. https://doi.org/10.1130/GES00523.1
Zhou H, Chen L, Sun Y, et al. (2012) Detrital zircon LA-ICP-MS ages of tertiary sandstones from western Qaidam basin:constraints on the uplift of Altun mountains. Acta Geologica Sinica 86(6): 906-922.
Zhuang G (2011) Insights into Cenozoic tectonics and climate change in northern Tibetan Plateau from basin analysis, thermochronology and isotopic study. University of California, Santa Cruz. p 152.
Zhuang G, Hourigan JK, Ritts BD, et al. (2011b) Cenozoic multiple-phase tectonic evolution of the northern Tibetan Plateau: Constraints from sedimentary records from Qaidam basin, Hexi Corridor, and Subei basin, northwest China. American Journal of Science 311: 116-152. https://doi.org/10.2475/02.2011.02